JSMPM

JOURNALS OF SUSTAINABLE MATERIALS PROCESSING AND MANAGEMENT
e-ISSN: 2821-2843

Vol. 6 No. 1 (2026) 20-28
https://publisher.uthm.edu.my/ojs/index.php/jsmpm

# Finite Element Analysis of 20×20 ft Container Flat Wagon Underframe Structure Using S355J2 Steel

**Dwiyan Boy Sandi Pratomo[1], Hedi Purnomo[2], Yoyok Winardi[1], Fadelan[1], Rizal Arifin[1]***

[1] *Department of Mechanical Engineering, Faculty of Engineering, Universitas Muhammadiyah Ponorogo, Jl. Budi Utomo No. 10, Ponorogo, 63471, INDONESIA*
[2] *PT Industri Kereta Api, Jl. Yos Sudarso No. 71, Madiun, 63122, INDONESIA*

*Corresponding Author: rarifin@umpo.ac.id
DOI: https://doi.org/10.30880/jsmpm.2026.06.01.002

**Article Info**

Received: 26 February 2026
Accepted: 26 March 2026
Available online: 15 May 2026

**Keywords**

Flat wagon, finite element method, S355J2, von Mises stress, safety factor, static loading

**Abstract**

The underframe is the key structure support to the floor of the railway cargo carriage and adherence to its stability is also crucial for operational safety in railroads. The paper is aimed at substantiating the strength of the underframe of a 2×20 ft container flat wagon fabricated from S355J2 structural steel via finite element methods. A convergence test for mesh discretization showed that 21 mm with a skewness value of 0.87 will be sufficient for numerical simulation. Various loadings were used according to the standard EN 12663-2, i.e., normal, lateral, axial compressive, axial tensile, and their combination. The maximum von Mises stress under combined loads was 217.79 MPa, which is smaller than the 355 MPa material yield stress. The EN 12663-2 maximum overall deformation of 7.5 mm was within the limit of 61.38 mm. The safety margin of 1.63 % has been computed, which falls within the accepted values of 1.5–2.0 and this means that the design of the underframe is sound for use in service conditions.

## 1. Introduction

A key part of modern logistic systems, and a contributor to the global economic infrastructure, is freight railway transport which has been in existence for a long period [1]. Rail transportation is considered better than road transportation because it lowers the cost of shipping over long lengths (more than 350 km), saves money on fuel, and reduces carbon dioxide emission [2]. Among the types of electric haulage in this case and that is electric rail freight, it is the one that has the least effect on the environment, almost succeeding with diesel trains by up to 26% carbon consumption [3]. Nevertheless, the railway infrastructure is still poor and obsolete. Most of the reinventions are not involved in sensitizing the intended Customer on reasons for change [4]. The cost of investments required for the acquisition of a better and advanced approach to rail freight practices and infrastructure has always found opportunities to reinvigorate investments and sensible changes in the systems [5]. To overcome these factors, there are specific interventions in four main areas which are typically considered when introducing rail reforms: investment, herd management, regulatory frameworks and new technologies and innovations [5]. It should be no secret that it is the rage with rail automation performers in cargo shipment and transportation and distribution management [6]. The quests are the proportionate capability to adhere to rail transport instead of trucks, the dedication and enthusiasm of the players and the willingness of competent citizens to participate in the market reforms [7]. Clearly defined pricing schemes, redevelopment of infrastructure and implementation of private public partnerships, are critical for the sustainability of rail freight services in a competitive environment [5,8]. In such a situation the integration of rail in modern logistics the integration of rail freight in the context of modern logistics is a function of shrewd technology application and effective policy [9].

Railways vehicles being body frames are required to meet stringent conditions which involve high strength-to-weight ratio, during collapse its ability to absorb energy without affecting its structural integrity, as well as different kinds of loads it expects to experience [10,11]. For example, in mechanically prepared formats, standards such as EN 12663-1:2015 confirm what all is needed superiority are performance criteria with regards to the car body which includes: bulletins about longitudinal compression, vertical or lateral loads and [11]. The assurance of structural adequacy requires a long way of tests such as proof loading of longitudinal elements of car body structure, triaxial test on rail vehicle sides, fatigue strength tests, etc., for each part under consideration [10]. Materials are discovered with the vehicle body until it is proved by testing, for instance tensile loading tests, and application to support elements on load of elements under fatigue is performed [10]. Reproduced from stainless steel for a long time, the car body was progressively replaced by aluminium alloys and fiber-reinforced polymers (FRPs) that assist in making glass-fiber- or GFRP-reinforced composites lighter while remaining safe for use [10,12]. Aluminium is still the main metal, because of favorable specific strength, resistance to corrosion and ease of fabrication of this material, while magnesium alloys can lower total car weight by another 10% [11]. FRP composites offer high specific strength and stiffness allowing to reduce the mass of the structure by 28–35% as compared to other metallic structures of the same purpose [11,12]. Nevertheless, one notable restraint removes that advantage with the recent advances in the processing of woven composites, and the problem becomes the fatigue life of structures with welded aluminum joints [13]. During the process of development, prototyping, and manufacturing, adherence to all these requirements is ensured by elaborate quality control procedures and norms, which include but are not limited to first article inspection (FAI) [14].

Finite element analysis (FEA) has become an indispensable approach in assessing the structural integrity of railway freight wagon underframes components that bear the primary mechanical demands imposed by both train equipment and transported cargo [15]. In one notable study, Yoon et al. [15] applied FEA to evaluate a newly designed freight car underframe fabricated from SM490A and ASTM A441 steels, with the aim of characterizing stress distribution patterns under maximum load conditions before physical testing commenced. Their experimental program encompassed vertical and compressive load tests, deflection measurements, and natural frequency assessments, with FEA results serving as the basis for optimal strain gauge placement [15].

The structural validation of underframes under varying weight conditions remains a fundamental requirement in freight wagon design. Addressing this need, Shukla et al. [16] utilized MSC Patran/Nastran to analyze a freight bogie bolster subjected to vertical forces, emergency braking loads, and lateral track excitations through transient analysis. By integrating artificial neural networks with genetic algorithms in an optimization framework, their approach yielded approximately 7.6% weight reduction while preserving fatigue strength, as confirmed through Goodman diagram evaluation [16]. In a related effort, Baykara [17] investigated Y25 bogie suspension systems under varying freight-loading scenarios using ANSYS based FEA, demonstrating that both stress and displacement responses remained within acceptable material thresholds throughout all tested conditions [17]. Collectively, these studies affirm that FEA represents a powerful and versatile methodology for advancing the design of freight wagon underframes, enabling simultaneous improvements in structural integrity, weight efficiency, and operational safety [15-17].

Structural steel S355J2 is classified as a low-carbon steel containing approximately 0.15% carbon and 1.46% manganese which makes it suitable for manufacturing yet able to withstand heavy structural use [18]. This steel grade is specifically employed for the underframe construction of freight trains manufactured by PT Industri Kereta Api Indonesia (PT INKA), a state-owned rolling stock manufacturer in Indonesia [18]. The underframe functions as the main load-bearing element of railway wagons by supporting all equipment and cargo during their operational period [15]. To the best of our knowledge, no previous research has investigated the flat wagon underframe which uses S355J2 structural steel to support two 20-foot container loads according to EN 12663-2 testing standards despite the existence of multiple studies about freight wagon structural analysis. Existing studies have predominantly focused on different wagon typologies, alternative materials, or single-container configurations, which leaves this design inadequately described through its stress patterns, overall physical changes, and safety factors for structural integrity. The present study conducts a static structural analysis of a 2×20 ft container flat wagon underframe using FEM to evaluate whether the S355J2 underframe design meets the structural safety requirements stipulated by EN 12663-2.

## 2. Methods

### 2.1 Geometry Modeling

The underframe geometry of the 2×20 ft container flat wagon was modeled in three dimensions using Autodesk Inventor 2020, based on engineering drawings provided by PT Industri Kereta Api Indonesia (PT INKA). The model showed all components of the underframe system which included the center sill and cross members and side sills and bolster elements. The publication does not reveal specific dimensional details about the underframe model because those measurements belong to a confidential engineering document that PT INKA owns. The team used simplification methods to reduce computational costs by removing nonstructural elements which included small fillets and holes before they entered the simulation environment.

## 2.2 Material Properties

The specified underframe material required S355J2 structural steel obtained to the EN 10025-2 standard. The S355J2 steel has the following mechanical properties: Material density of 7 850 kg/m3, Young's modulus of 210 GPa, Poisson's ratio of 0.30, yield strength of 355 MPa, and ultimate tensile strength in the range of 470 -630 MPa. In the simulation software, the material properties of S355J2 were specified as isotropic and linearly elastic.

## 2.3 Finite Element Modeling

All structural simulation was carried out using ANSYS R1 2022. The geometry was discretized into tetrahedral elements, and mesh convergence was confirmed in which the element size was successively reduced until the difference in maximum von Mises stress between one mesh to the next fell below 5%. The process of finalizing the mesh involved selecting a mesh with acceptable criteria of skewness.

## 2.4 Boundary Condition and Loading

All boundary conditions and loading scenarios were implemented in accordance with EN 12663-2:2010 for freight wagon structures. The remote displacement supports (A, B, C, and D) illustrate the bogie connection points in Fig. 1 controlled the underframe movement. Fig. 1 illustrates the four loading configurations applied to the underframe in accordance with EN 12663-2, where boundary constraints at bogie connection points A–D are held constant across all scenarios. In Fig. 1a, vertical forces of 85,280 N are applied downward at each of the six-corner casting points E–J to simulate the static weight of two fully loaded ISO 20 ft containers. Lateral forces of 89,226 N acting horizontally are shown in Fig. 1b, representing curve-induced and track excitation loads. Fig. 1c and Fig. 1d depict longitudinal compressive and combined loading scenarios respectively, with the combined case (Fig. 1d) representing the most critical operational condition as required by the standard.

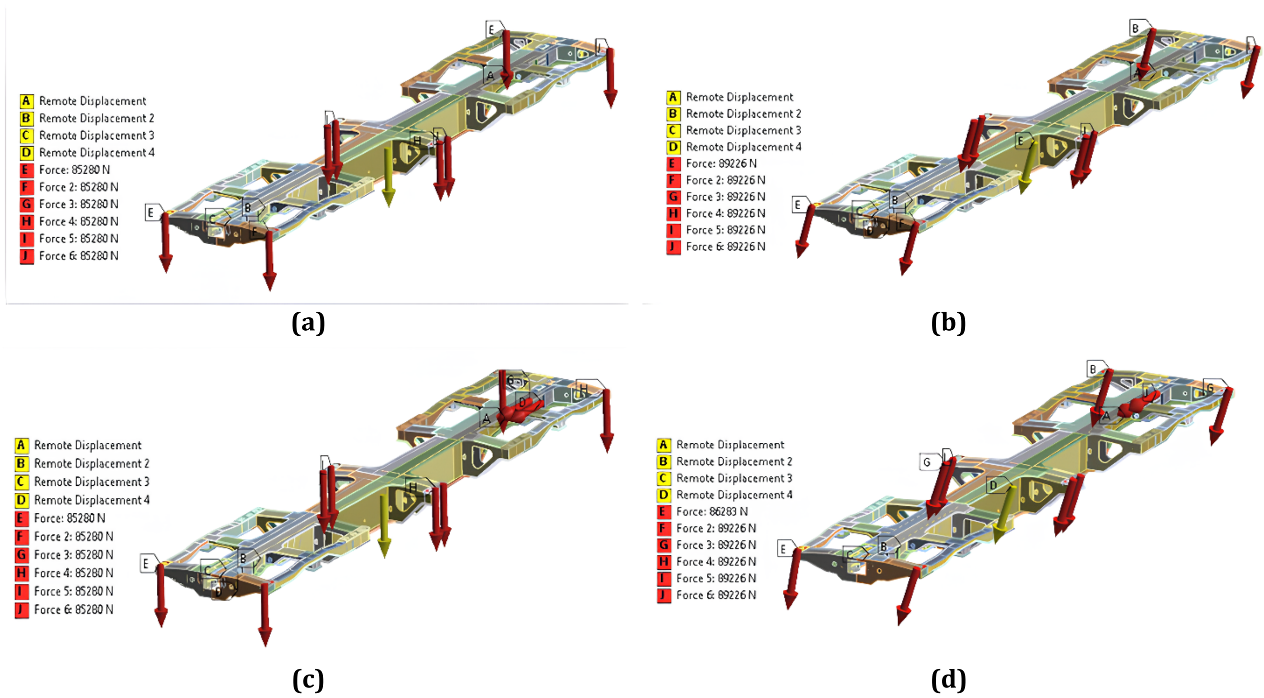


**Fig. 1** *Loading configurations applied to the 2×20 ft container flat wagon underframe (a) vertical load of 85,280 N at each corner casting point E–J; (b) lateral load of 89,226 N at points E–J; (c) longitudinal load of 85,280 N at points E–J; (d) combined load of 86,283 N at point E and 89,226 N at points F–J. Remote displacements A–D represent the bogie connection constraints applied in all scenarios*

The loading forces were derived from the operational conditions of a flat wagon carrying two ISO 20 ft containers. The two containers reached their total payload capacity because each container could hold a maximum weight of 24,000 kg. The gravitational force equivalent is 48,000 × 9.81 = 470,880 N which distributes itself across six corner casting points E–J per container configuration. The vertical loading point received 470880 N total force which distributed itself equally to six points resulting in 85280 N force. The total vertical load of 47,088 N per bogie produced a lateral force which was calculated as 10% of that load and that force distributed across six points which resulted in 89,226 N per point according to EN 12663-2 requirements. The combined load scenario showed that the dominant longitudinal point E carried 86,283 N because of force vector superposition while the remaining points F–J maintained a lateral value of 89,226 N.

The researchers studied four different loading scenarios which are displayed in Fig. 1. (i) The first scenario used vertical loading (Fig. 1a) which simulated the weight of two fully loaded 20 ft containers that were distributed throughout six corner casting locations (E–J) with each location experiencing an 85,280 N force. (ii) The second scenario used a lateral force (Fig. 1b) which applied an 89,226 N horizontal force that moved across the wagon's body from position E to position J to create simulations of lateral track excitation and curve-induced forces during operation. (iii) The third scenario applied a longitudinal load (Fig. 1c) which simulated shunting and braking conditions through compressive and tensile forces of 85,280 N distributed across six loading points (E–J) along the wagon's longitudinal axis, while the opposite end was constrained. (iv) The fourth scenario used combined loading (Fig. 1d) which involved simultaneous application of vertical and lateral and longitudinal compressive loads that included an 86,283 N force at point E and an 89,226 N force at points F to J which created the major operational condition required by EN 12663-2.

### 2.5 Structural Evaluation Criteria

The evaluation of structural performance required three testing criteria which included the following: (1) maximum von Mises stress, which must remain below the material yield strength of 355 MPa; (2) total deformation, which must not exceed 0.5 mm per 100 mm of span length (equivalent to 61.38 mm for the full underframe length of 12,276 mm); and (3) safety factor, calculated as the ratio of yield strength to maximum von Mises stress, which must fall within the acceptable range of 1.5–2.0, as required by EN 12663-2.

## 3. Results and Discussion

### 3.1 Mesh Convergence Study

The researchers conducted a mesh convergence study before their structural analysis. The study determined that finite element results remained constant regardless of the mesh density used. Numerical solutions reach convergence in finite element analysis when mesh size decreases and element count increases. The simulation results reached convergence when maximum von Mises stress and total deformation showed less than 5% change between two consecutive mesh refinements. Table 1 shows how researchers measured maximum von Mises stress and total deformation through their experiments which used element sizes ranging between 25 mm and 19 mm. The maximum stress difference between the 21 mm and 20 mm meshes met the convergence criteria because it remained under 5% threshold.

**Table 1** *Mesh convergence test results*

| Element size (mm) | Stress (MPa) | Deformation (mm) | Skewness |
|---|---|---|---|
| 25 | 109.5 | 5.4 | 8.88 |
| 24 | 123.6 | 5.4 | 8.88 |
| 23 | 122.5 | 5.5 | 0.84 |
| 22 | 133.9 | 5.5 | 0.99 |
| 21 | 134.9 | 5.5 | 0.87 |
| 20 | 135.6 | 5.5 | 0.99 |
| 19 | 136.7 | 5.5 | 0.92 |

In this analysis, the skewness metric was used for an estimate of mesh quality since this is a standard that serves with a defined threshold below which it can be assumed that acceptable mesh characteristics were satisfied and skewness should remain below 0.9 as this metric gives added insight into how far an element's shape has deviated from what would be expected for its design [20]. The results of the mesh convergence analysis indicated that 21 mm was chosen as the best performing size as it met a skewness measurement of 0.87 at which point simulations rendered an acceptable quality standard of less than 0.9.

## 3.2 Vertical Loading Condition

The vertical loading is performed for all the above conditions and is simulated as a sum of static weight (the combined weight of two fully loaded ISO 20ft containers) and self-weight from the underframe structure. A total of 53,500 kg was to be examined with a weight underframe of 5.5 tonnes plus two containers (24 tonnes each) above for which the total gravitational force acting on eight corner casting points through a load of 524,835 N creates Ø 65,604 N point load. The von Mises stress and total deformation contours under vertical load conditions are shown by scientists in Fig. 2a and Fig. 3a respectively. The highest value of von Mises stress was recorded to be 179.32 MPa, which extended through both the upper and lower longitudinal beams, and cross beams along with the mid-section up to the underframe. Its value is still well below S355J2 yield strength (YP = 355 MPa). The maximum total deformation of 7.0 mm occurred between two bogie pivot points and is well below the limit of 61.38 mm according to standard EN 12663-2.

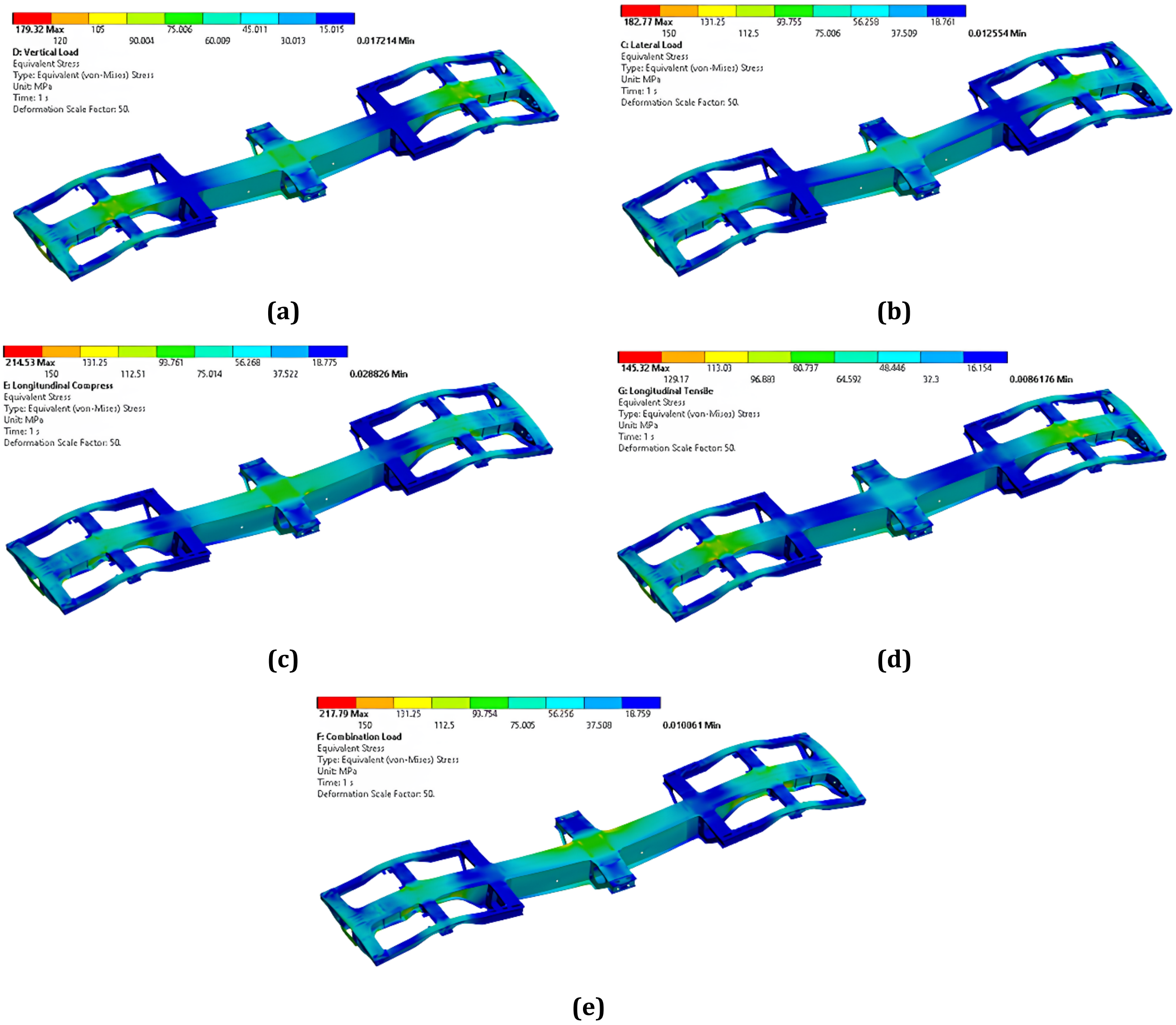


**Fig. 2** *Von Mises stress contours of the 2×20 ft container flat wagon underframe under (a) Vertical load; (b) Lateral load; (c) Longitudinal compressive load; (d) Longitudinal tensile load; (e) Combined load*

## 3.3 Lateral Loading Condition

In this case, lateral loading was performed using horizontal forces to represent the side loads resulting from maneuvering on-track and slight impacts as described by EN 12663-2. The von Mises stress indicates its distribution by total deformation contours presented in Fig. 2b and Fig. 3b. Maximum von Mises stress reported during lateral loading was 182.77 MPa, being located on the side parts of main longitudinal beam where cross beams are connected to it. While the value was slightly higher than vertical loading results, it remained far below yield strength of the material which was 355 MPa. Due to that being the highest measurement of deformation collected at any point in time, through any testing condition, no more than 7.5 mm total deformation was recorded.

This required slight adjustments in the strapping but did not exceed deformation limits; Characteristic deformation across lateral crossbeam member boundaries, excluding attachment points and outliers, remaining well within EN 12663-2 (deformation under load) defined limit of 61.38 mm.

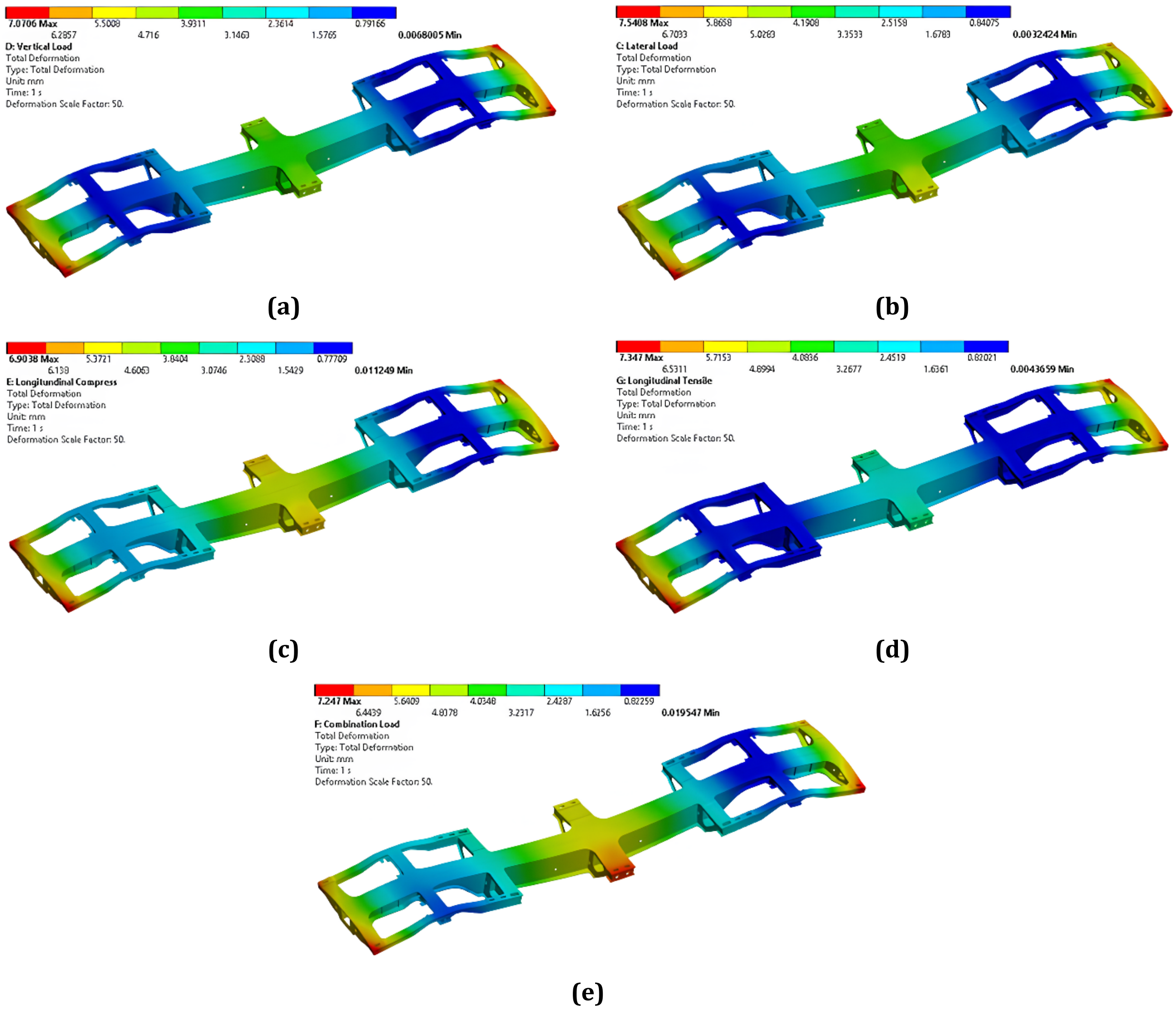


**Fig. 3** *Total deformation contours of the 2×20 ft container flat wagon underframe under: (a) Vertical load; (b) lateral load; (c) Longitudinal compressive load; (d) Longitudinal tensile load; (e) Combined load*

## 3.4 Longitudinal Loading Condition

For the longitudinal loading scenario, two tests were performed: 1) compressive loading with a buffing force of 2,000 kN (i.e. shunting impact) and 2) tensile loading with a draft force of 1,500 kN (i.e. braking and acceleration), applied at the coupler end frame area per EN 12663-2. Figure 6 presents the stress and deformation contours drawn from compressive loading. 2c and 3c, and under tensile loading in Fig. 2d and Fig. 3d.

Finding the maximum von Mises stress under long axial compressive loading reached 214.53 MPa which was obtained representing the highest recorded stress among all tested load cases. This occurred due to the bending force from the applied end load, which caused stress concentration to occur at both ends of the longitudinal beams and just above the center pivot bogie area. The maximum deformation was 6.9 mm in total. Under longitudinal tensile loading, the maximum von Mises stress of 145.32 MPa was less than the maximum measurement since stress concentrated at the mid-body cross members and maximum deformation reached 7.3 mm. 355 MPa yield strength served as limitation in that all of the stress recorded for both sub-cases were below and complied with EN 12663-2 permissible boundaries.

J. of Sustainable Materials Processing and Management Vol. 6 No. 1 (2026) p. 20-28

### 3.5 Combined Loading Condition

The loading test applied vertical and lateral and longitudinal compressive forces which generated the most dangerous operational test conditions in accordance with the standards of EN 12663-2. Tests of von Mises stress and total deformation are depicted in Fig. 2e and Fig. 3e.

At four torsional and bending scenarios, the maximum von Mises stress under combined loading was 217.79 MPa at the location of interaction between a main longitudinal beam with cross beams connecting an interframe midspan and a center-pivot bogie mounted on top of a main beam. This value is the highest stress measured during loading tests and it is used for calculating safety factors. The maximum total deformation of 7.2 mm occurred under combined loading and was located at the cross beam ends in the middle section and at the crossbeams in both underframe ends. The results of the study indicate that all observed deformations were elastic, since in all stress measurements, maxima did not exceed yield strength –355 MPa. The safety factor (FoS) was calculated using the following Equation (1):

$$FoS = \frac{Stress\ limit}{Max. von\ Mises\ stres} = \frac{355\ MPa}{217.79\ MPa} = 1.63 \quad (1)$$

The value satisfies the safety factor required by EN 12663-2 [7], which states that a safety factor between 1.5 and 2.0 must be obtained, thus confirming that the design condition which limits the project has been successfully achieved. Table 2 shows the overview of all loading tests related to the EN 12663-2 acceptance criteria. This led to parameters of safety factor values calculated for combined loading condition at maximums value of von Mises stress and deformation are 217.79 MPa and 7.5 mm, respectively (Fig. 2e and Fig. 3e). All loading conditions satisfy both the compliance standards of stress and deformation.

**Table 2** *Comparison of simulation results with EN 12663-2 acceptance criteria*

| Loading condition | Maximum von Mises stress (MPa) | Stress limit (MPa) | Maximum deformation (mm) | Deformation limit (mm) |
|---|---|---|---|---|
| Vertical | 179.32 | 355 | 7.0 | 61.38 |
| Lateral | 182.77 | 355 | 7.5 | 61.38 |
| Longitudinal (compressive) | 214.53 | 355 | 6.9 | 61.38 |
| Longitudinal (tensile) | 145.32 | 355 | 7.3 | 61.38 |
| Combined | 217.79 | 355 | 7.2 | 61.38 |

### 3.6 Discussion

The structural performance verification of S355J2 subframes of 2×20 ft container flat wagons has been carried out using FEA, and all EN 12663-2 criteria have been met. Under the dominant and combined loading, a maximum von Mises stress of 217.79 MPa reached is only equal to 61.4 % of material yield strength value which indicates that the material has still enough potential to elongate until rupture occurs (355 MPa). In this study shows the results that match previous research conducted by Satrijo and Prahasto where it was found 188 MPa (58.8% utilization) [21] in a freight underframe with 320 MPa yield strength and Rayendri et al. in a PPCW's flat wagon [22] found 231.7 MPa (71.3% utilization). Results indicate stress utilization in the present study is comparable to predicted values for well-designed freight wagon structures. While aluminum alloys and FRP composites offer weight advantages, their practical limitations, including fatigue degradation at welded aluminum joints [13] and the high cost and poor field repairability of FRPs [12,14], make them less suitable for heavy freight wagon underframes in an industrial manufacturing context like PT INKA. S355J2 steel, by contrast, offers well-established weldability, ductile and predictable failure behavior, and straightforward in-service repairability [18], while the 31% margin between the peak stress observed in this study (217.79 MPa) and the material's minimum ultimate tensile strength (470 MPa) provides a meaningful safety reserve that alternatives struggle to match.

For the individual loading cases, the maximum stress state of 214.53 MPa occurred in longitudinal compressive loading while the combined load case reached its peak level of stress at 217.79 MPa. Unsurprisingly, the stress concentrations identified were located where load transfer would occur, at the interfaces between main longitudinal beams and cross beams, above the center pivot bogie. The results of the study revealed that PT INKA needs to guarantee weld quality and material integrity in these areas during manufacturing processes.

The greatest deformation of 7.5 mm, noted during lateral loading, reached 12.2% of the permitted value limit of 61.38 mm according to EN 12663-2. The study found that all resulting deformations were elastically behaved, thus no change in the ISO container corner fittings dimensions would be observed under such form of loading during the wagon service life. These findings support PT INKA to begin the production for the customized flat wagon design requested by their customer, with a safety factor of 1.63 on the governing combined loading that maintains structural integrity while offering well-optimized and efficient material use. The maximum stress of 217.79 MPa, representing only 61.4% of the yield strength, indicates that the underframe operates well within the elastic range, which for structural steel generally corresponds to fatigue lives exceeding $10^6$ cycles, equivalent to many years of normal freight service [16,20]. Nevertheless, the identified stress concentration zones at the longitudinal beam–cross beam interfaces and the center-pivot bogie region should be prioritized in routine inspection programs [15], and future work incorporating dynamic and cyclic fatigue analysis is recommended to fully assess long-term service performance [16].

## 4. Conclusion

The study presents structural performance assessment of a container flat wagon underframe constructed from S355J2 structural steel by means of finite element analysis under different service-related load conditions. The study covered four separate loading conditions defined by EN 12663-2, including vertical and both lateral and longitudinal as well as combined loading tests. The loading tests also showed that under combined loading conditions, the maximum von Mises stress reached only 217.79 MPa which was still lower than the material yield strength (355 MPa). Maximum total deformation of 7.5 mm was observed during lateral loading, which remained within the EN 12663-2 maximum allowable limit of displacements of up to 61.38 mm. The safety factor of 1.63 obtained from combined loading tests was also within the acceptable range of 1.5 to 2.0. The results proved that the structural integrity of the S355J2 underframe design by fulfilling all EN 12663-2 operational safety requirements which even includes carrying two ISO 20 ft containers. The current study must be extended through future studies which shall cover dynamic load conditions along with fatigue analysis under cyclic operational loads and shunting impact loading not covered in this research work.

## Acknowledgement

The authors would like to acknowledge PT Industri Kereta Api (PT INKA), Madiun, Indonesia, and in particular the granted access to the computational hardware and software necessary for performing the finite element simulations presented in this study. The authors declared the following potential conflicts of interest with respect to the research, authorship and/or publication of this article: The authors used Paperpal (AI academic writing tool by Editage) for English proof reading and editing manuscript during preparation of this manuscript.

## Conflict of Interest

Authors declare that there is no conflict of interests regarding the publication of the paper.

## Author Contribution

*The authors confirm their contribution to the paper as follows:* ***study conception and design:*** *D.B.S.P., H.P., Y.W., R.A.;* ***data collection:*** *D.B.S.P., H.P.;* ***analysis and interpretation of results:*** *D.B.S.P., Y.W., F., R.A.;* ***draft manuscript preparation:*** *D.B.S.P., R.A. All authors reviewed the results and approved the final manuscript.*

## References

[1] Comtois, C. (2017). Rail Transport: Freight. International Encyclopedia of Geography (pp. 1–6). https://doi.org/10.1002/9781118786352.wbieg0242

[2] Prabowo, R. (2017). The Optimization of Railway Transportation Modes to Reduce Costs and Support Logistics Activities. Global Research on Sustainable Transport (GROST 2017), 480-490. https://doi.org/10.2991/grost-17.2018.41

[3] Merchan, A. L., Belboom, S., & Léonard, A. (2020). Life cycle assessment of rail freight transport in Belgium. Clean Technologies and Environmental Policy, 22(5), 1109-1131. https://doi.org/10.1007/s10098-020-01853-8

[4] Zhang, A. (2016). Proceedings of the 2016 International Conference on Economics, Social Science, Arts, Education and Management Engineering, 515–519. https://doi.org/10.2991/essaeme-16.2016.109

[5] Pisa, N. (2021). Innovations to Improve Rail Freight Efficiency: Considerations for Emerging Economies. Journal of Contemporary Management, 18(1), 223–242. https://doi.org/10.35683/jcm20093.103

[6] Xyugan, W., & Lysochenko, A. A. (2023). Improving the Supply Chain Management of China's Rail Logistics System. E3s Web of Conferences, 403, 07030. https://doi.org/10.1051/e3sconf/202340307030

[7] Rong, C., Li, X., Zhang, G., & Wang, X. (2025). Analysis on the adjustment of transportation structure and the logistics transformation of railway freight. Railway Sciences, 4(1), 82-96. https://doi.org/10.1108/rs-09-2024-0040

[8] Gurzhii, A. V., Timashov, V. O., & Veselov, M. Y. (2024). The tariff regulation of railway freight transportation in EU. Analytical and Comparative Jurisprudence, (6), 550–554. https://doi.org/10.24144/2788-6018.2024.06.89

[9] Buthphorm, O., Sukhotu, V., & Hengsadeekul, T. (2024). An analysis of the development factors of rail freight transport in Thailand: a structural equation modeling approach. Infrastructures, 9(7), 102. https://doi.org/10.3390/infrastructures9070102

[10] Lee, W. G., Kim, J.-S., Sun, S.-J., & Lim, J. (2016). The Next Generation Material for Lightweight Railway Car Body Structures: Magnesium Alloys. Proceedings of the Institution of Mechanical Engineers Part F Journal of Rail and Rapid Transit, 232(1), 25–42. https://doi.org/10.1177/0954409716646140

[11] Cascino, A., Meli, E., & Rindi, A. (2025). Design and optimization of a hybrid railcar structure with multilayer composite panels. Materials, 18(21), 5013. https://doi.org/10.3390/ma18215013

[12] Jagadeesh, P., Puttegowda, M., Oladijo, O. P., Lai, C. W., Gorbatyuk, S., Matykiewicz, D., Rangappa, S. M., & Siengchin, S. (2022). A Comprehensive Review on Polymer Composites in Railway Applications. Polymer Composites, 43(3), 1238–1251. https://doi.org/10.1002/pc.26478

[13] Saifudin, S., Muhayat, N., Surojo, E., Manurung, Y. H., & Triyono, T. (2022). Mitigation of Porosity and Residual Stress on Carbody Aluminum Alloy Vibration Welding: A Systematic Literature Review. Automotive Experiences, 5(3), 477–493. https://doi.org/10.31603/ae.7965

[14] Pascu, C. I., Gheorghe, S., Popa, D., & Popa, O. (2018). Aspects about the quality control at first article inspection (FAI) for parts obtained by materials composites used in the railway sector. Advanced Engineering Forum, 27, 262–267. https://doi.org/10.4028/www.scientific.net/aef.27.262

[15] Yoon, S. C., Kim, Y., Kim, J. G., Park, S. H., & Lee, H. U. (2013). A Study on the Structural Fracture of Body Structure in Railroad Car. Key Engineering Materials, 577–578, 301–304. https://doi.org/10.4028/www.scientific.net/kem.577-578.301

[16] Shukla, S. K., Gupta, R., & Vyas, N. S. (2010). Weight Reduction in an Indian Railway CASNUB Bogie Bolster Considering Fatigue Strength. International Journal of Vehicle Structures and Systems, 2(3–4). https://doi.org/10.4273/ijvss.2.3-4.03

[17] Baykara, C. (2025). Investigation of Mechanical Strength and Deformation Properties of Y25 Bogie Suspension Systems by Finite Element Analysis. Railway Sciences. https://doi.org/10.1108/rs-04-2025-0010

[18] Irwansyah, A. A., Syukron, M., Setyani, A., & Santoso, M. (2024). Analysis of Primary Coating Thickness Effects on Adhesion Strength in S355J2+N Steel Material. Journal of Metallurgical Engineering and Processing Technology, 5(1), 78. https://doi.org/10.31315/jmept.v5i1.12796

[19] Robert D. C., David S. M., Michael E. P., & Robert J. W. (2021). Concepts and Applications of Finite Element Analysis (4th ed.). Wiley.

[20] Hibbeler, R. C. (2017). Mechanics of Materials (10th ed.). Pearson.

[21] Satrijo, D., & Prahasto, T. (2012). Analisis Kekuatan Under Frame Kereta Barang Menggunakan Metode Elemen Hingga. ROTASI, 9(3), 1–5. https://doi.org/10.14710/rotasi.9.3.1-5

[22] Rayendri, K. A., Satrijo, D., & Kurdi, O. (2023). Desain Dan Analisis Gerbong Datar (Ppcw) Kereta Api Dengan Metode Elemen Hingga. Jurnal Teknik Mesin, 11(2), 145-146.